ISSN 0965-5441, Petroleum Chemistry, 2016, Vol. 56, No. 2, pp. 151–157. © Pleiades Publishing, Ltd., 2016.
Original Russian Text © M.L. Pavlov, D.A. Shavaleev, B.I. Kutepov, O.S. Travkina, I.N. Pavlova@c, R. A. Basimova, A.S. Ershtein, I.M. Gerzeliev, 2016, published in Neftekhimiya, 2016, Vol. 56, No. 2, pp. 171–177.

Synthesis and Investigation of ZSM-5 Zeolite-Based Catalysts for Benzene Alkylation with Ethylene

M. L. Pavlov[a], D. A. Shavaleev[b], B. I. Kutepov[c], O. S. Travkina[c], I. N. Pavlova[c], R. A. Basimova[a], A. S. Ershtein[b], and I. M. Gerzeliev[d]

[a]*OOO Salavatnefteorgsintez Scientific and Technical Center, ul. Molodogvardeitsev 30, Salavat, 453256 Bashkortostan, Russia*

[b]*PAO Salavatneftekhimproekt, ul. Gagarina 8, Salavat, 453256 Bashkortostan, Russia*

[c]*Institute of Petroleum Chemistry and Catalysis, Russian Academy of Sciences, pr. Oktyabrya 141, Ufa, 450075 Bashkortostan, Russia*

[d]*Topchiev Institute of Petrochemical Synthesis, Russian Academy of Sciences, Leninskii pr. 29, Moscow, 117912 Russia*

e-mail: ink@anrb.ru

Received August 20, 2015

Abstract—A catalyst for alkylation of benzene with ethylene to ethylbenzene has been prepared by mixing 70% H^+-ZSM-5 zeolite having a silica ratio of 30 with 30% pseudoboehmite followed by shaping granules, their drying, and calcining for 6 h at 650°C in air. A part of the catalyst has been treated by steaming with 100% steam at 600°C for 3 h. The physicochemical and catalytic properties of catalyst samples have been studied. The catalysts have been tested in a laboratory setup in the temperature interval of 380–450°C at 2.5 MPa, a benzene space velocity of 15 h^{-1}, and a benzene/ethylene molar ratio of 7 : 1. The properties of EBEMAX-1, an imported analogue of the catalysts have been studied under the same conditions. It has been found that the synthesized catalysts are not inferior to the imported sample in the catalytic properties.

Keywords: ZSM-5 zeolite, catalyst, steaming, alkylation, benzene, ethylene, ethylbenzene

DOI: 10.1134/S0965544116020110

The majority of modern developments in the field of benzene alkylation with ethylene are dedicated to the design and application of heterogeneous catalysts, which are solid, porous multicomponent systems containing an active component (zeolite) and matrix (binder). Zeolites of the ZSM-5, ZSM-11, mordenite, USY, β, MCM-22, MCM-49 types are used as an active component. The matrix can be Al_2O_3, SiO_2, amorphous aluminosilicate or mixture of a these substances. After mixing all of the components, granules of specified size are formed from the mixture by different methods and subsequently subjected to thermal treatment (drying and calcining). In some cases, the catalyst is subjected to further modification. The zeolite content in the catalysts usually makes 60 to 80 wt % [1–11].

Because of a relatively small pore diameter of ZSM-5 and ZSM-11 zeolites [12], which is 0.5–0.6 nm and is comparable with the size of the benzene molecule (5.9 nm), the benzene molecule can be inserted only in the excited state into the molecular-sieve structure of these zeolites. This condition is achieved only at high temperatures (above 300°C) when the benzene alkylation reaction with ethylene occurs in the gas phase.

The ethylbenzene production process via gas-phase benzene alkylation with ethylene, as implemented at Gazprom Neftekhim Salavat under license of the Groznyi Research Institute [13], uses the foreign zeolite catalyst EBEMAX-1 manufactured by Suüd-Chemie. Therefore, investigations aimed to create a domestic catalyst for this process are especially demanding at the moment.

EXPERIMENTAL

The catalysts were prepared using powdered ZSM-5 zeolite with a silica ratio of 30 manufactured by Ishimbai Specialized Chemical Catalyst Plant (ISKhZK). The H^+form of the zeolite was prepared by ion exchange in an aqueous ammonium nitrate solution at 80–90°C, an NH_4^+ in solution to Na^+ in zeolite cations ratio of 1.5 eq/eq, pH 5.5–7.0, and 1-h duration of each treatment. There were three repeated treatments. Then, the zeolite was washed with distilled water, dried, and calcined in air at 600°C for 6 h. The X-ray powder diffraction pattern of an H^+ZSM-5 zeolite was characterized by the presence of intensive diffraction peaks at the angles of 7.92°, 7.94°, 8.78°, 8,89°, 13.95°, 14.77°, 23.08°, 23.25°, 23.40°, 23.82°,

Table 1. Particle size composition of powdered H^+-ZSM-5 zeolite

Entry	Range of values					
Crystal size, μm	0.1–0.5	0.5–2.0	2.0–4.0	4.0–6.0	6.0–8.0	8.0–10.0
Weight fraction, %	0.45	36.32	44.55	17.47	1.20	0.01

and 23.96° inherent in the ZSM-5 zeolite only [14], indicating high phase purity of the product obtained.

Pseudoboehmite available from the same manufacturer was used as the binder in the catalyst preparation.

The catalyst was prepared by the following way: the H^+ZSM–5 zeolite was mixed with pseudoboehmite in the 70 : 30 weight ratio. The blend was shaped into granules by extrusion, dried, and calcined at 650°C in air for 6 h (Cat-1). Then, a portion of the catalyst was additionally subjected to steaming at 600°C for 3 h (Cat-2).

The chemical composition of the samples was analyzed using the complexometric titration and flame photometry techniques [15, 16]. The phase composition of the zeolite and catalysts was determined on a Philips PW 1800 automatic diffractometer using monochromated Cu-K_a radiation in the 2θ angle region of 5° to 40° with a step size of 0.5 grad/min and a counting time of 20 s per step. The IR spectra of zeolite-containing materials were recorded in KBr disks on a Bruker VERTEX 70v instrument over the scanning range of 4000 to 400 cm^{-1} with 4 cm^{-1} resolution. The particle size of the powdered zeolite was determined by the diffraction (scattering) of laser radiation ($\lambda = 680$ nm) by dispersed-phase particles distributed in a dispersing medium. The morphology of zeolite crystals was studied on a Jeol JSM-6490 LV electron microscope at an accelerating voltage of 20–30 kV with different magnifications (500, 2000, 5000, 10000).

The characteristics of the porous structure of the catalysts were determined by the nitrogen low-temperature adsorption–desorption (LADN) method using a Micrometrics ASAP-2020 sorptometer. Before the analysis the samples were evacuated at 350°C for 6 h. The BET specific surface area was calculated at a relative partial pressure of $P/P_0 = 0.2$; the pore size distribution was determined from the desorption curve using the BJH (Barrett–Joyner–Halenda) method; and the total pore volume was found by the BJH method at $P/P_0 = 0.95$. The micropore volume in the presence of mesopores was determined by de Boer and Lippens t-method [17]. The porous structure of the catalysts was characterized using the mercury porosimetry (MP) method with a Prosimeter-2000 instrument. Before testing, the samples were evacuated at 25°C for 4 h. The intrusion pressure was varied from 1 to 1900 atm. The contact angle of mercury was 141.3° [17]. From the measurement results, the specific surface area, the pore volume, the average pore radius, and pore size distribution were calculated . The pore size distribution was calculated in terms of the cylindrical pore model [17], and the specific surface area was taken as the total surface area of all model cylinders.

The equilibrium adsorption capacity of the catalysts for water, benzene, and heptane vapors was determined using the desiccator method at $P/P_0 = 0.8$ and 25°C. The acid properties of the zeolite and catalysts were investigated by the temperature-programmed desorption of ammonia (TPD NH_3) [18].

The catalytic properties of the samples were tested in the benzene alkylation reaction with ethylene to form ethylbenzene (EB) in laboratory a flow reactor unit. The reactor (10 mm in diameter and 120 mm in height) was charged as follows: porcelain packing in an amount of 25 cm^3 was placed at the bottom, and 5 cm^3 of the catalyst was disposed on this bed and covered by porcelain packing.

Testing was performed in the temperature range of 380 to 420°C at a pressure of 2.5 MPa, a benzene space velocity of 15 h^{-1}, and a benzene/ethylene molar ratio of 7 : 1.

The products were analyzed on a Kristallyuks 4000 gas chromatograph with a flame ionization detector using a 60 m × 0.32 mm × 1.0 μm fused silica capillary column coated with ZB-1. The data were processed on a software and hardware system using the internal normalization method.

The catalytic properties of catalyst samples were characterized in terms of benzene (B) conversion and ethylbenzene (EB) selectivity.

The benzene conversion (C_B, %) was calculated by the equation: $C_B = 100\ (c_{in}{}^B - c_{ex}{}^B)/c_{in}{}^B$, where $c^B{}_{in}$ is the weight fraction of benzene in the feed, wt % and $c_{ex}{}^B$ is the weight fraction of benzene in alkylate, wt %. The ethylbenzene selectivity (S^{EB}, %) was characterized in terms of the relative concentration of ethylbenzene in the products: $S_{EB} = 100 c_{ex}{}^{EB}/C_B$.

RESULTS AND DISCUSSION

The results of the study of the particle size composition of the powdered H^+ ZSM-5 zeolite show that about 80% of crystals have a size of 0.5 to 4.0 μm (Table 1).

Since the amount of coarse crystals is relatively low, it may be stated that fine zeolite has been used for preparing the catalyst. The results of a scanning electron microscopy study of the H^+ZSM-5 zeolite morphology show (Fig. 1) that zeolite particles differ in both

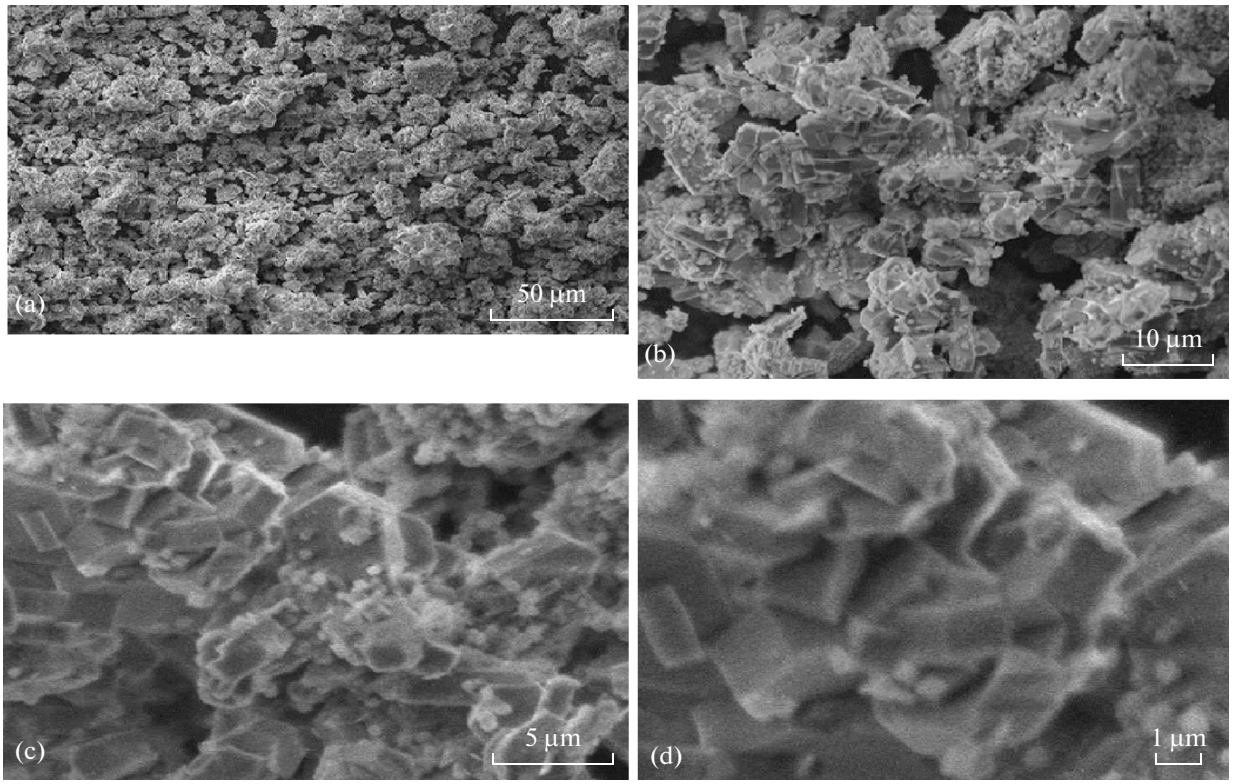

Fig. 1. Electron microscopic images of powdered H^+-ZSM-5 zeolite (a, b, c, d) at 500, 2000, 5000, and 1000 magnifications, respectively.

form (because of the presence of crystal aggregates) and size of the crystals, the size of which is consistent with the data obtained by studying the particle size composition of the zeolite.

Catalysts Cat-1 and Cat-2 differ little from each other in chemical composition. The Al_2O_3 content is ~34%, SiO_2 makes ~66%, and the amount of Na_2O does not exceed 0.04 wt %.

The X-ray diffraction patterns of Cat-1 and Cat (Fig. 2) show only the ZSM-5 zeolite and γ-Al_2O_3 phases. Besides, the diffraction peaks of Cat-1 are more intense, indicating partial amorphization of the zeolite in Cat-2 after steaming.

Figure 3 depicts IR spectra of catalysts Cat-1 and Cat-2. In the spectrum of Cat-2, the frequency of the fundamental band of asymmetric stretching vibrations of the first type (1110 cm^{-1}), i.e. the vibrations inside TO_4 tetrahedrons, remains unchanged. This shows the presence of tetrahedrally coordinated aluminum in the lattice after steaming.

The porous structure of catalyst granules consisting of the blend of zeolite and γ-Al_2O_3 crystals is a complex system. The zeolite is characterized by the microporous structure, and γ-Al_2O_3 is mesoporous. In addition, a secondary porous structure is formed between the zeolite and γ-Al_2O_3 crystals. Thus, the pore volume of catalyst granule is made by these three components. Table 2 shows the equilibrium adsorption capacity of the H^+ ZSM-5 zeolite and catalysts based on it for water, benzene, and heptane vapors.

The adsorption capacity of the catalysts for water vapor is significantly lower than that for benzene and heptane vapors. The difference is explained by the presence of mesopores in catalyst granules; in the mesopores, these hydrocarbons undergo transition into the liquid state because of capillary condensation and the water vapor does not.

After steaming (Cat-2), the water vapor adsorption capacity falls because of partial destruction of the zeolite framework and, as a result, a decrease in the micropore volume. The pore volume in terms of water uptake by the catalysts is higher than the adsorption capacity for the hydrocarbons because of the presence of macropores in catalyst granules.

Figure 4 illustrates similarity in form of the isotherms of nitrogen adsorption–desorption on catalysts Cat-1 and Cat-2.

At a relative pressure (P/P_0) of 0 to 0.05, the isotherms exhibit a sharp rise typical of microporous coals and zeolites [17]. At pressures of 0.45 to 1.0, there is a hysteresis loop due to a broad size distribution of mesopores. When P/P_0 reaches ~0.98, a sharp rise of the isotherms begins again, which is associated with the presence of macropores in the catalysts.

The size distribution of mesopores in the catalysts ranges widely from 2 to 60 nm, having a maximum in

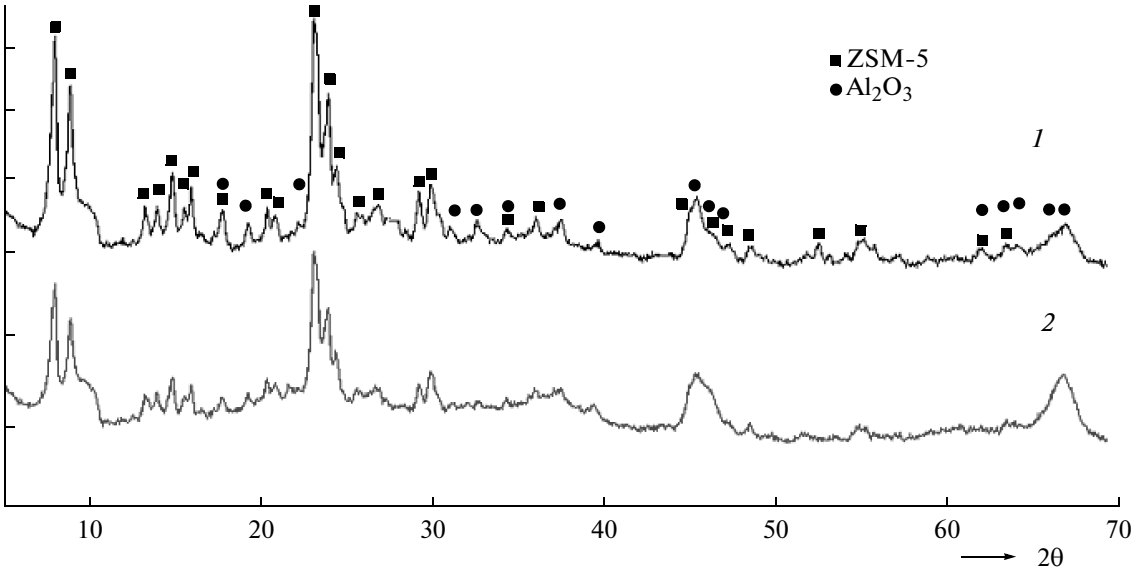

Fig. 2. XRD patterns of catalysts (*1*) Cat-1 and (*2*) Cat-2.

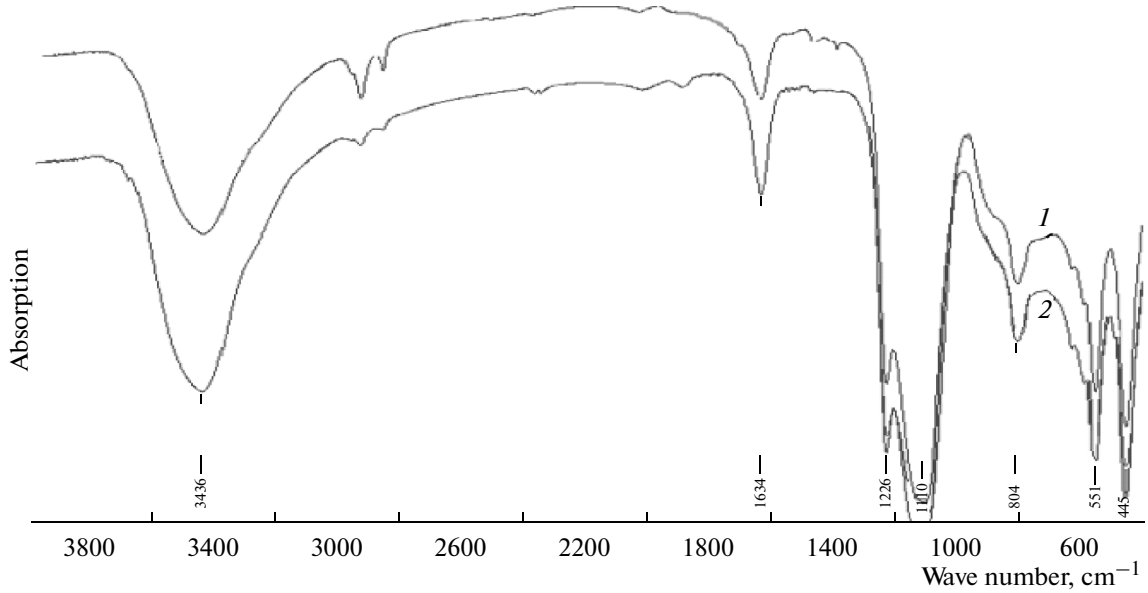

Fig. 3. IR spectra of catalysts (*1*) Cat-1 and (*2*) Cat-2.

at 4–6 nm (Fig. 5). The presence of the maximum of this region is due to γ-Al_2O_3 used as a binder. Steaming has almost no effect on the pore size distribution range in the catalyst. Table 3 gives characterization of the porous structure of the catalyst by the BET (nitrogen) and (mercury) porosimetry methods.

Steaming insignificantly decreases the specific surface area from 273 to 268 m^2/g and increases the mesopore volume from 0.266 to 0.309 cm^3/g by virtue of partial amorphization of the zeolite in the catalyst (Cat-2). In addition, the secondary porous structure (meso- and macropores) of the catalysts is characterized in this table according to the mercury porosimetry data. After steaming (Cat-2), the total pore volume increases because of the transformation of part of mesopores into macropores.

The results of the TPD NH_3 investigation of the acid properties of the zeolite and catalysts are presented in Table 4.

The total concentration and the concentration of the "strong" and "weak" acid sites are substantially lower in the catalyst containing 30% binder (Cat-1) than in the powdered H^+ZSM-5 zeolite. Steaming (Cat-2) decreases the concentration of acid sites even

Table 2. Adsorption capacity of zeolite and catalysts

Material	Equilibrium adsorption capacity (cm^3/g) for vapor			Pore volumes by water absorption, cm^3/g
	H_2O	C_6H_6	C_7H_{16}	
H^+-ZSM-5	0.13	0.16	0.18	–
Cat-1	0.11	0.30	0.38	0.67
Cat-2	0.09	0.27	0.37	0.66

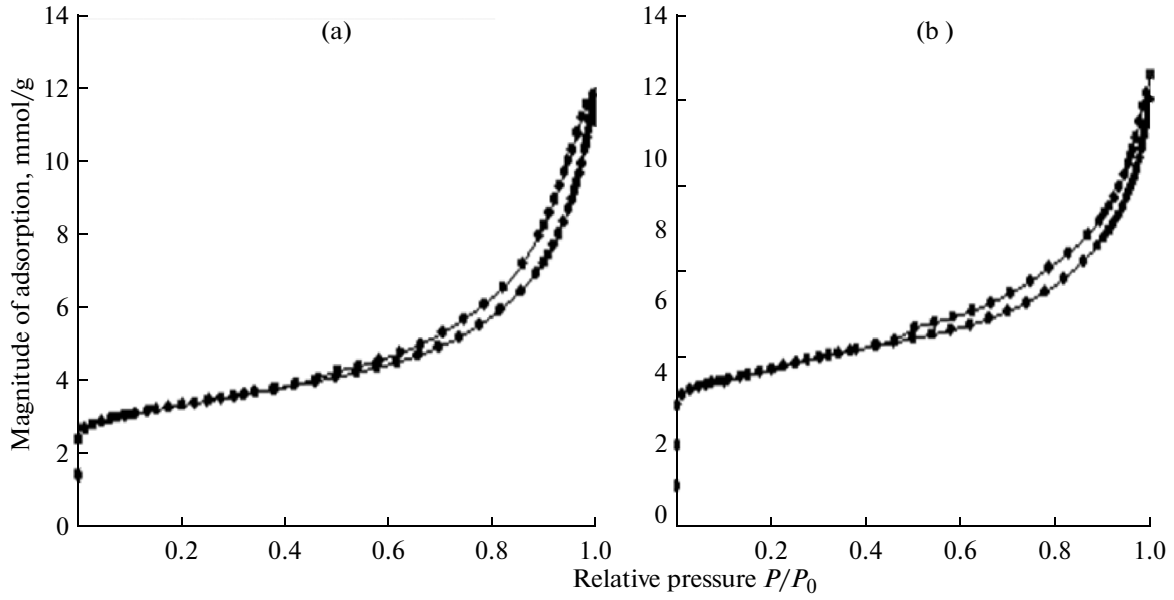

Fig. 4. Adsorption–desorption isotherms of nitrogen on catalysts (a) Cat-1 and (b) Cat-2.

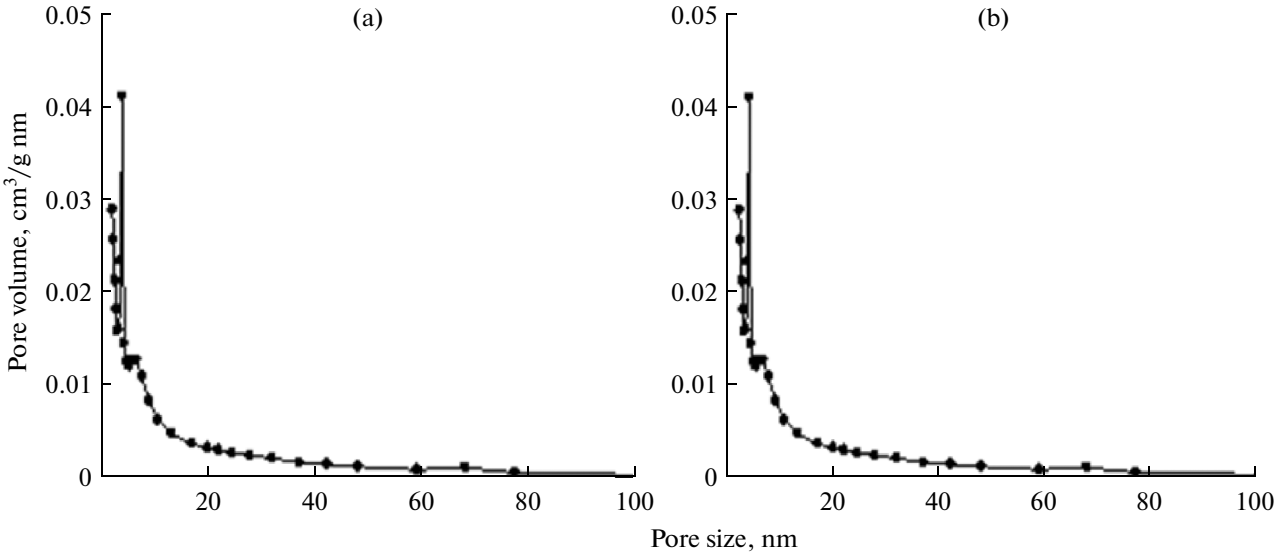

Fig. 5. Size distribution of mesopores for catalysts (a) Cat-1 and (b) Cat-2 as calculated by the BJH method.

Table 3. Characterization of the porous structure of catalysts

	Parameter	Catalyst	
		Cat-1	Cat-2
LADN method	**Micro- and mesopores**		
	BET specific surface area, m^2/g	273	268
	Pore volume, cm^3/g		
	less than 1 nm	0.110	0.090
	more than 1 nm	0.266	0.309
	Average pore diameter, nm	7.9	8.2
	Specific surface area, m^2/g	51.4	68.1
MP method	**Meso- and macropores**		
	Pore volume, cm^3/g in pore radius interval, nm		
	less than 50	0.254	0.217
	50–100	0.411	0.540
	more than 100	0.035	0.040
	total	0.700	0.797
	Average pore diameter, nm	50.0	50.0

Table 4. Acid properties of zeolite and catalysts (TPD NH_3 method)

Material	Acid properties, μmol NH_3/g		
	"weak" acid sites	"strong" acid sites	total acidity
H^+-ZSM-5	284	186	470
Cat-1	199	130	329
Cat-2	63	18	81

more, with the decrease being especially noticeable for the strong acid sites.

Table 5 shows the results of testing the catalytic properties of the synthesized catalysts and the imported catalyst (ImpC) in the benzene alkylation reaction with ethylene.

As the reaction temperature increases from 380 to 420°C, the benzene conversion, the EB concentration in the alkylate, and the selectivity for EB increases on all of the catalysts.

Of the catalysts tested, Cat-1 turns to be the most active. As is shown above, the catalyst acidity decreases after steaming (Cat-2), a change that definitely leads to some decline in activity in comparison with Cat-1.

In the benzene alkylation reaction with ethylene, undesirable impurities, such as xylene isomers, propylbenzene (PB), ethyltoluene, diethylbenzenes (DEB), and polyalkylbenzenes (PAB), are produced, but their amount is within the permissible limits. The maximal amount of these impurities is formed on catalyst Cat-1. Note that the amount of xylene isomers on the foreign catalyst and Cat-1 increases with an increase in the reaction temperature, whereas it remains almost unchanged and has a minimal value (~0.01 wt %) on Cat-2.

Table 5. Comparison of catalytic properties of catalysts

Parameter	Feed-stock	Temperature, °C								
		380						420		
hydrocarbon composition, wt %		ImpC	Cat-1	Cat-2	ImpC	Cat-1	Cat-2	ImpC	Cat-1	Cat-2
		alkylate								
Pre-benzene fraction	0.05	0.33	0.08	0.14	0.39	0.11	0.12	0.27	0.07	0.12
Benzene	99.86	86.36	82.54	85.54	85.57	81.46	82.79	85.04	81.30	81.40
Toluene	0.03	0.07	0.08	0.050	0.07	0.09	0.05	0.07	0.11	0.05
Ethylbenzene	0.00	11.30	14.50	11.75	12.41	15.80	14.34	13.18	16.50	16.20
PB	0.00	0.07	0.28	0.15	0.05	0.23	0.13	0.05	0.20	0.09
Σ Xylenes	0.00	0.01	0.03	0.01	0.01	0.04	0.01	0.02	0.06	0.01
Ethyltoluene	0.00	0.07	0.14	0.15	0.04	0.09	0.10	0.04	0.06	0.05
Σ DEB	–	1.72	2.16	2.09	1.41	1.99	2.32	1.26	1.47	1.94
PAB	0.06	0.07	0.19	0.13	0.06	0.20	0.15	0.08	0.23	0.14
Total	100	100	100	100	100	100	100	100	100	100
Benzene conversion, %	–	13.5	17.3	14.3	14.0	18.4	17.1	14.8	18.6	18.5
EB selectivity, %	–	84	84	82	87	86	84	89	89	88

Thus, the catalysts synthesized in this study are highly competitive in catalytic properties with the foreign counterpart.

REFERENCES

1. T. F. Degnan, Jr., C. M. Smith, and C. R. Venkat, Appl. Catal., A **221**, 283 (2001).
2. C. Perego and P. Ingallina, Green Chem. **6**, 274 (2004).
3. M. West and F. S. Abdo, US Patent No. 5157180 (1992).
4. J. Chen, US Patent No. 5866736 (1999).
5. J. T. James Merrill and J. R. Butler, US Patent No. 5955642 (1999).
6. H. K. C. Timken, A. W. Chester, S. C. Ardito, and M. P. Hagemeister, US Patent No. 6596662 (2003).
7. H. K. C. Timken, A. W. Chester, S. C. Ardito, and M. P. Hagemeister, US Patent No. 6747182 (2004).
8. C. B. Curt Campbell, T. V. Harris, P. Tequi, and J.-L. Le Coent, US Patent No. 7109141 (2006).
9. M. N. Rogov, Kh. Kh. Rakhimov, O. L. Elin, et al., RU Patent No. 2256640 (2005).
10. M. N. Rogov, Kh. Kh. Rakhimov, M. Kh. Ishmiyarov, et al., RU Patent No. 2265482 (2005).
11. M. N. Rogov, Kh. Kh. Rakhimov, M. Kh. Ishmiyarov, et al., RU Patent No. 2265483 (2005).
12. G. T. Kokotailo, US Patent No. 4 229 424 (1980).
13. I. M. Gerzeliev, S. I. Myachin, I. D. Tasueva, and S. N. Khadzhiev, Pet. Chem. **49**, 59 (2009).
14. *Collection of Simulated XRD Powder Patterns for Zeolites,* Ed. by M. M. J. Treacy and J. B. Higgins (Elsevier, Amsterdam, 2001), 4th ed.
15. N. S. Poluektov, *Flame Photometry Analysis Methods* (Goskhimizdat, Moscow, 1959) [in Russian].
16. G. Charlot, *Les méthodes de la chimie analytique: Analyse quantitative minérale* (Masson, Paris, 1961).
17. A. P. Karnaukhov, *Adsorption: Texture of Disperse and Porous Materials* (Nauka, Novosibirsk, 1999) [in Russian].
18. A. N. Khazipova, I. N. Pavlova, N. G. Grigor'eva, et al., Khim. Tekhnol., No. 1, 5 (2012).

Translated by K. Aleksanyan